RSC Advances

ROYAL SOCIETY OF CHEMISTRY

www.rsc.org/advances

Carbon monoxide interactions with pure and doped $B_{11}XN_{12}$ (X=Mg, Ge, Ga) nano-cluster: A theoretical study

Alireza Soltani*[a], Masoud Bezi Javan[b]

[a]Clinical Research Development Unit (CRDU), Sayad Shirazi Hospital, Golestan University of Medical Sciences, Gorgan, Iran

[b]Physics Department, Faculty of Sciences, Golestan University, Gorgan, Iran

Abstract

The goal of this work is study of the novel sensor for detecting the toxic gas compounds of CO by $B_{11}XN_{12}$ (X= Ge, Mg, and Ga) nano-clusters in terms of its energetic, geometric, and electronic structure using DFT calculations at PBE-D method. The reaction of the CO gas with these doping atoms results a weak interaction and an elongation of X-N bond of the $B_{11}XN_{12}$ nano-clusters. After the adsorption of the CO gas over doped positions of $B_{11}XN_{12}$ nano-cluster, the conductivity of the adsorbent and the atomic charges in some of near B and N atoms around X atoms are dramatically enhanced. These calculations represent the capabilities of the $B_{11}XN_{12}$ nano-clusters in designing novel materials based on $B_{11}XN_{12}$ for potential applications as gas sensor.

Keyword: DFT, CO, $B_{12}N_{12}$ nano-cluster, Doping, Gas sensors

* Corresponding author. E-mail: Alireza.soltani46@yahoo.com, Tel: +98-938-4544921

1. Introduction

Carbon monoxide or CO is an extremely poisonous gas to human and animal bodies when encountered in concentrations above 35 ppm. It is known a colourless poisonous gas with no smell which can be as one of the most fatal gases with a significant role in the air pollutants and in human daily life. Owing to increase the concern over the safety and healthy hazards related to this gas, there is an increasing demand of CO sensors.[1-3] Since, theoretical studies over the adsorption and dissociation of CO molecule toward the Rh-decorated SWCNT,[4] Fe-$B_{18}N_{18}$ cluster,[5] Al-graphetic boron nitride sheet,[6] Al/Ga-doped BN nanotube,[7] FeCo alloy (110) surface ,[8] ZnO (1010) surface,[9] $B_{12}N_{12}$ nano-cage,[10] doped h-BN monolayer,[11] and transition metal doped BN nanotube [12] were reported. In particular, theoretical studies have shown that some metal-doped BN nanostructures were proposed as promising candidates for chemical sensors.[13-17] During the last decade, various kinds of BN-based nanostructures consists of the nanotubes, nanohorns, nanoparticles, nano sheets, and nano-cages, have attracted considerable attention owing to their unique chemical and physical properties.[18-20] $B_{12}N_{12}$ is one of the stable known class of small III-V nano-clusters with the network of B-N bonds, which is energetically favorable. The 4-membered rings of $B_{12}N_{12}$ consists of the B-N bonds which are resulted in angular strainin the network. Since, B_iN_i clusters have been widely investigated both theoretically and experimentally.[21-26] Recently, Oku etal. [27] have synthesized $B_{12}N_{12}$ detected by laser desorption time-of-flight mass spectrometry. Their research indicated that BN nano-clusters is a structure built from 4 squares and 6 hexagons rings. For example, Matxain and co-workers theoretically studied the electronic structure and the energy differences between covalent and van der Waals dimers using the hybrid B3LYP and MPW1PW91 density functional theory.[28] Li et al. perposed bonding character and electronic structure of $B_{12}C_6N_6$ fullerene by using *ab initio*

calculations .[29] They found that replacing N atom with C atom in the $B_{12}N_{12}$ nano-cage results a decrease of the cluster energy gap. Bahrami and co-authors repoted a theoretical study of amphetamine adsorption upon the pure, P-, and Al-doped $B_{12}N_{12}$ nano-cage at the M06-2X/6-311++G** level of theory.[30] Based on their results, the pure $B_{12}N_{12}$ nano-cage has a better condition for detecting of amphetamine compared with P- and Al-doped $B_{11}N_{12}$ nano-cage. Doping in BN nanomaterials can alter its electronic properties outstandingly, which extremely develop its sensing applicability. In the previous reports, many studies indicated that the reaction of different molecules with the pure and doping metal BN nanostructures by using DFT calculations.[31-33] In this work, we investigated the interaction of CO molecule with the pure, Ga, Ge, and Mg atoms of $B_{11}XN_{12}$ nano-clusters to find whether these adsorbents can be used as a gas sensor in environmental monitoring using DFT calculations.

2. Computational details

In order to study of the structural parameters and electronic properties of the pure and $B_{11}XN_{12}$ (X= Ge, Mg, and Ga) nano-cluster interacted with CO molecule, we carried out density functional theory (DFT) calculations. The goal is calculating equilibrium geometries, adsorption energies, Mulliken population charge analysis (MPA), molecular electrostatic potential (MEP), frontier molecular orbital (FMO), and density of states (DOS) analyses for these complexes. All the geometry optimizations and energy calculations were performed using GAMESS software [34] at the level of density functional theory (DFT) using PBE functional augmented with an empirical dispersion term (PBE-D) and 6-311G** standard basis set. Also the corresponding optical adsorption spectra were obtained through time-dependent density functional theory (TD-DFT) calculations in the gas phase regime.[35-37] The relaxed structures were further subjected to

the computations for harmonic vibrational frequencies at the PBE functional. For all systems, the SCF convergence limit was set to 10^{-6} a.u. over energy and electron density. The basis set superposition error (BSSE) for the adsorption energy was corrected implementing the counterpoise method.[38,39] The adsorption energies (E_{ad}) of each structures were determined at 298.15 k and 1 atm using the formula:

$$E_{ad} = E_{B12N12\text{-}CO} - (E_{B12N12} + E_{CO}) + E_{BSSE} \quad (1)$$

$$E_{ad} = E_{B11XN12\text{-}CO} - (E_{B11XN12} + E_{CO}) + E_{BSSE} \quad (2)$$

where $E_{B11XN12\text{-}CO}$ is the total energy of the $B_{11}XN_{12}$ nano-cage interacting with the CO molecule. $E_{nano\text{-}cage}$ and $E_{TM\text{-}nano\text{-}cage}$ are the total energies of the pure and $B_{11}XN_{12}$, respectively, and E_{CO} is the total energy of an isolated CO molecule. The electrophilicity index (ω) concept was stated for the first time by Parr et. al.[40,41] Chemical potential (μ) is defined according to the following equation:

$$\mu = -\chi = -1/2(I+A) \quad (3)$$

electronegativity (χ) is defined as the negative of chemical potential, as follows: $\chi = -\mu$. According to koopmans theorem,[42] chemical hardness (η) can be approximated by below equation:

$$\eta = 1/2\,(I-A) \quad (4)$$

I ($-E_{HOMO}$) is the ionization potential and ($-E_{LUMO}$) the electron affinity of the molecule. Where E_{HOMO} is the energy of the highest occupied molecuar orbital and E_{LUMO} is the energy of the lowest unoccupied molecular orbital of the considered structure. Softness (S) and electrophilicity index are determined as the following equations, respectively.

$$S = 1/2\eta \quad (5)$$

$$\omega = (\mu^2/2\,\eta) \quad (6)$$

3. Results and discussion

First of all, we optimized the $B_{12}N_{12}$ nano-cage as an adsorbent for detection of CO molecule at the gas phase using PBE-D method and 6-311G** standard basis set (see Fig. 1). Then, we considered two stable states of the CO adsorption, which locates from its C and O heads over top of a B atom of $B_{12}N_{12}$ nano-cage. When the CO molecule is adsorbed from C and O heads toward the boron atom of the adsorbent, the adsorption energies and distances of CO physisorption are -0.27 eV (**II**: 1.655 Å), and -0.06 eV (**III**: 3.176 Å) respectively (Table 1). Regarding to previous studies the adsorption of CO molecule over (5, 5) SWCNT and capped CNT in their most stable states are about -0.147 and -0.02 eV.[1,43] Baierle et al. and Beheshtian et al. showed that the BN nanotubes have physical interactions with the CO molecule in the range of about -0.13 and -0.06 eV.[13, 44] In the agreement with our results also, Beheshtian and co-workers have reported DFT study of the CO molecule in reaction with $B_{12}N_{12}$ nano-cluster.[10] They have shown that the CO can be adsorb over the nano-cluter with the adsorption energy of 0.15-0.30 eV. It was found that the length of C≡O bond (1.1386 Å at the PBE-D) after reaction with the $B_{12}N_{12}$ is slightly smaller than those of free CO molecule (1.357 Å), which is close to the reported experimental value of 1.128 Å.[45] By Mulliken charge analysis, a charge transfer at about 0.172e (C head) and 0.019e (O head) occures from CO molecule (electron donor) to $B_{12}N_{12}$ nano-cluster. In Fig. 1, we explored the density of states for the above discussed different CO-adsorption over the $B_{12}N_{12}$ nano-cluster. Compared with DOS of the pristine nano-cluster, the adsorption of CO molecule alters the electronic structure of $B_{12}N_{12}$, as shown in Fig. 1. It indicates a remarkable change (**II**) of energy gap (E_g) about 45.8%. Since the DOS plots of the complex clearly reveals that the LUMO level has a distinct change after the adsorption process.

<Fig. 1>

<Table 1>

In this stage, first, we have used the optimized structures and density of states of the perfect $B_{12}N_{12}$ nano-cluster with doped transition metal atoms containing Mg, Ge, and Ga to calculate the adsorption of CO molecule as shown in Fig 2. The length of Mg-N, Ge-N, and Ga-N bonds of doped nano-cluster are calculated with values of 2.079, 1.946, and 1.921 Å, respectively. In a similar study, Li et al. represented that a structure is generated by replacing N with C atom in the $B_{12}N_{12}$ nano-cage by using ab initio calculations.[29] Soltani et al.[16] has indicated that the length of Ga-N bond of $B_{11}XN_{12}$ nano-cage is about 2.072 Å. As reported in Table 2, the angle of N-Mg-N, N-Ge-N, and N-Ga-N bonds of $B_{11}XN_{12}$ nano-cluster were found to be about 69.66, 76.92, and 79.76˚, respectively. As shown in Fig. 2, all of the doped systems with the Mg, Ge, and Ga atoms in the $B_{11}XN_{12}$ nano-cluster are belong to the C_s point group, while $B_{12}N_{12}$ nano-cage point group symmetry is T_h.[46] In $B_{11}XN_{12}$ nano-cluster, metal atoms move slightly out of the cluster form as lead to a significant change of the local geometry of the nano-cluster. The point charges over the Mg, Ge, and Ga atoms in $B_{11}XN_{12}$ nano-cluster are 0.621, 0.720, and 0.739e, while the corresponding values for N atoms are about -0.522, -0.512, and -0.503e, respectively. To better understand the properties of crucial transition states for X-doped $B_{11}XN_{12}$ nano-cluster, we have plotted frontier molecular orbital (HOMO and LUMO) for these systems that these orbitals play an important role in governing many chemical reactions, and also they are responsible for charge transfer properties (see Fig. 3). By comparison, it is found that the HOMO and LUMO energy levels can be significantly changed due to doping atoms as the energy gap of the nanoclusters reduces in process of CO adsorption. From HOMO and LUMO analysis, it is easily seen that the uniformly shift of the HOMO level to the upper energy region due to the

mutual charge transfer and the interaction between N atoms of the nano-cluster and dopant atoms.

<Fig. 2>

<Fig. 3>

<Table 2>

In the next stage, we choosed to search the suitable nano-cluster for CO detection. After full optimization, adsorption states of CO molecule over the X-doped $B_{12}N_{12}$ nano-cluster using PBE method was studied and reported in Table 3. This method has shown to get reasonable results for dative B-N bonds in comparison with other methods.[47] In these interactions (Figs. 4, 5, 6), CO molecule has electrostatic contact with the X-doped $B_{12}N_{12}$ nano-clusters. The observed trend for the $B_{11}GaN_{12}$ nano-cluster with CO molecule is found to be **III**>**II**>**IV**>**I**. In contrast, these values in the $B_{11}MgN_{12}$ is found to be **III**>**I**> **II** > **IV**, which means that the $B_{11}MgN_{12}$ is more stable than that of the $B_{11}GaN_{12}$, whereas CO molecule is physisorbed toward $B_{11}GeN_{12}$ nano-cluster, which mainly stemmed from the van der Waals interaction, as it can be seen in Table 3. According to the relative energy values, $B_{11}GeN_{12}$ is the least stable among all of interacted species with the CO molecule. The minus value of adsorption energy in the interaction between adsorbent and adsorbate, representing that the CO molecule configuration very weak physical bond with the doping atoms of the nano-cluster. Due to the weak type of interactions between adsorbate and adsorbent can be remarkable in gas detection because such ineffective interactions represent that desorption of the adsorbate could be easy and the divice can suffer from short recovery times.[48] If the E_{ad} is significantly decreased, much shorter recovery time is expected. $\tau = \upsilon_0^{-1} e^{(-E_{ad}/k_BT)}$, where T is tempreture , k_B is the Boltzmanns constant (8.62×10^{-5} eV K^{-1}), and υ_0 is the attempt frequency. According to this equation, $B_{11}XN_{12}$ nano-cluster should be good CO

sensors with qiuick response as well as short recovery time. Upon the interaction of the CO molecule with X-doped $B_{12}N_{12}$ nano-cluster, the Mg-N, Ga-N, and Ge-N bond lengths shift to 2.098, 1.938, and 1.890 Å, respectively, resulting change in hybridization from sp^2 to sp^3. As a result, the adsorption of CO over the $B_{11}GaN_{12}$ and $B_{11}MgN_{12}$ nano-clusters leads to elongation of bond length but in the $B_{11}GeN_{12}$ is shortened bond-length (Table 2). Bahrami and co-workers studied the effects of Al and P-doped $B_{12}N_{12}$ nano-cage at the M06-2X method.[30] They have shown that the distance between the Al and the N atoms is about 1.97 Å. In addition, they reported that the adsorption of amphetamine on the surfaces of perfect Al- and P-doped $B_{12}N_{12}$ nano-cages are found at -1.63, -2.48, and -0.33 eV, respectively. The results of these reportes revealed that the Al-doped $B_{11}N_{12}$ can be used as an adsorbent in the environmental system.

<Fig. 4>

<Fig. 5>

<Fig. 6>

<Table 3>

For better understanding of the nature of CO adsorption over the electronic properties of adsorbent, we have carried out the electronic density of states (DOSs). GaussSum program was used to gain DOS results.[49] DOS spectrum of these structures represent the HOMO-LUMO gaps of the X-doped BN nano-clusters. E_g of Mg-, Ga-, and Ge-doped $B_{12}N_{12}$ nano-clusters are 3.14, 3.74, and 4.41 eV, while this value in the pure nano-cluster is about 5.0 eV. However, there is notecible change in the resistivity by decreasing the E_g for structures when compared to that of $B_{12}N_{12}$ nano-cluster. Oku and co-workers experimentally introduced that the energy gap of the pure $B_{12}N_{12}$ nano-cluster is about 5.1 eV between HOMO and LUMO.[27] Thus, the accuracy of the theoretical calculation is close to experimental data as mentioned above. In the most stable

configurations, after the CO adsorption toward the Mg, Ga, and Ge atoms of $B_{11}XN_{12}$ nano-clusters, ΔE_g of these configurations have significantly changed at about 54.14, 61.23, 46.82%, respectively. This result implies that the electronic properties of the $B_{11}GaN_{12}$ nano-cluster is very sensitive to the CO adsorption in comparison with the pure $B_{12}N_{12}$ nano-cluster. Zhang et al. found that the graphitic BN sheet (g-BN) that by replacing Al-dopant and defects have high sensitive to the CO gas compared to the pure model.[6] Also, their results indicated that the vacancy-defect g-BN has more change of energy gap than Al-dopant g-BN. As seen in Table 3, DOS spectrum in CO/ $B_{11}GaN_{12}$ complex (State **II**) near to both of the valance and conduction levels have distinct changes in comparison with that of the $B_{12}N_{12}$. In the CO/ $B_{11}GeN_{12}$ complex (State **II**), the valence level (-3.981 eV) of this complex has a distinct change when compared to that of $B_{12}N_{12}$ (-6.38 eV). DOS spectrum for CO/ $B_{11}GeN_{12}$ complex (State **I**) revealed that the conduction level (-4.42 eV) of this complex has a distincet change in comparison with that of $B_{12}N_{12}$ (-2.96 eV). This reports leads to a slight reduction in the work function that is important in the field emission applications. The values of Φ in the adsorption of CO gas , in the most stable models (Table 3), upon the Mg, Ga, and Ge atoms of $B_{11}XN_{12}$ nano-cluster are considerably decreased from 1.57, 1.87, and 2.21 eV to 0.72 (State **I**), 0.72 (State **II**), and 1.17 eV (State **II**), respectively. The decrement in the work function (Φ) values reveals that the field emission properties of the nano-clusters are more noticeable on the adsorption of CO gas as the electrons can be pulled from the surface more easily.[50,51] We provided in Fig. 7 the crucial excited states for CO molecule interacting with $B_{11}XN_{12}$ nano-cluster, where the electron cloud in their LUMO, LUMO+3, and LUMO+5 are dominated over the CO molecule, while in their HOMO orbitals have not the same distribution of the electron density. To explore the interaction mechanism between CO and $B_{11}XN_{12}$ nano-cluster, we studied molecular electrostatic potential

(MEP) maps for these processes where the positive charges over the X-doped $B_{12}N_{12}$ nano-cluster represents the blue colors (see Fig. 8). MEP plots computed at an isovalue of 0.0004 e/au^3. As demonstrated in these configurations the CO molecule with blue color (positive charge) acts as an electron donor in the adsorption process. Most negative and natural regions of the MEP plots are colored yellow and green, respectively. Table 4 implies to the values of the quantum molecular discriptors computed for the adsorption of CO gas toward the $B_{11}XN_{12}$ nano-cluster. When CO gas reacts with Mg-, Ga-, and Ge-doped $B_{12}N_{12}$ nano-cluster, the global hardness in position of Ga and Mg dopants have the highest amount of hardness while the lowest amount is in related to Ge dopant. In addition, when the CO gas interacts with the $B_{11}XN_{12}$ nano-cluster, the η values have significant gain from 1.87, 1.57 and 2.21 eV in Ga-, Mg, and Ge-doped $B_{12}N_{12}$ nano-cluster to 2.54 eV (**III**), 2.59 eV (**V**), and 2.56 eV (**V**) after the adsorption of CO, respectively (see Table 4). For the siutable species, $B_{11}GaN_{12}$/CO, the global hardness of complex is significantly increased and the electrophilicity of the complex is significantly reduced, indicating that the reactivity of complex is decreased and also indicating that the stability of the complex is increased.[52] The electrophilicity index of the Ga- Mg and Ge-doped $B_{12}N_{12}$ nano-clusters were higher than that of CO molecule, suggesting a charge transfer from adsorbate to adsorbent.[53-55]

<Fig. 7>

<Fig. 8>

<Table 4>

In addition, in order to investigate the stability of X-doped $B_{12}N_{12}$ nano-clusters, it is needful to calculate the harmonic frequencies for all of the adsorption models. The vibrational frequencies of the Mg-N, Ga-N, and Ge-N in $B_{11}XN_{12}$ nano-clusters are in region of 590, 610

and 562 cm^{-1}, respectively. IR vibrational spectrum indicates that two active vibration modes (B-N bond) of $B_{12}N_{12}$ in region of 755 and 1375 cm^{-1} at PBE-D method, indicating a good agreement with the corresponding theoretical values of 1294 and 825 cm^{-1} by Pokropivny et al.[56] and 1649 and 909 cm^{-1} by Jensen and Toftlund. [57] Calculations over CO/ $B_{11}MgN_{12}$ complex shows that the bond at 2190 cm^{-1} is assigned to C-O molecule while the values appearing at 1922 and 2159 cm^{-1} corresbonds to the C-O stretching mode (from C head) of the CO adsorbed over $B_{11}GeN_{12}$ and $B_{11}GaN_{12}$ nano-clusters, respectively.

Here, we use a TD-PBE/6-311G** calculation to study the optical properties of CO molecule interacting with $B_{11}XN_{12}$ nano-cluster.[58] In Table 5, we have presented the lowest excitation modes of the four most stable configurations of the adsorbing CO systems. For pure $B_{11}GaN_{12}$ systems, we have two considerable peaks in energies of 2.44 and 2.66 eV as they are related to the H-1->L and H-2->L vertical transitions. In this case the H->L transition has very low intensity which shows that the wave functions of the HOMO and excitation modes to the adsorption state. As for **I** and **IV** states the first excitation energy interval is between 2.54-2.85 eV while for **II** and **III** states the lowest excitation energy range is about 1.5 eV. In all considered CO adsorbed states the contribution of the H->L excitation has a noticeable growth. Similar trends also can be seen in corresponding Mg and Ge-doped systems. Although the lowest excitation modes have a red shift in comparison with Ga-doped BN nanocage. In these cases HOMO and LUMO have similar radial distribution on the cluster which results consequently low dipole moment and oscillation strength.

<Table 5>

4. Summary

We have carried out a density functional theory calculation over the adsorption of CO gas upon the Mg-, Ge-, and Ga-doped $B_{12}N_{12}$ nano-cluster. It is found that CO gas is weakly adsorbed over the $B_{11}XN_{12}$ nano-cluster owing to van der Waals interaction between CO and adsorbent. In addition, it is seen a slight reduction of the charge transfers in the adsorption process from CO to $B_{11}XN_{12}$ nano-cluster in comparison with the pure nano-cluster. From calculated results, we concluded that the electronic structure of the $B_{11}GaN_{12}$ has dramatic change after the CO adsorption process in comparison with the $B_{11}MgN_{12}$ and $B_{11}GeN_{12}$ nano-clusters. Besides, the $B_{11}GaN_{12}$ nano-cluster can act as a suitable sensor in detection of CO gas with significantly changing in the energy gap and work function of an adsorbent.

Acknowledgments

We should thank the Sayad Shirazi Hospital, Golestan University of Medical Sciences, Gorgan, Iran. We should also thank the Jaber Ebne Hayyan Unique Industry researchers Company, Gorgan city, Iran.

Refrences

1 K. Liao, V. Fiorin, D.S.D. Gunn, S.J. Jenkinsa, D.A. King, *Phys. Chem. Chem. Phys.*, 2013, **15**, 4059.

2 S. Lin, X. Ye, J. Huang, *Phys. Chem. Chem. Phys.*, 2014, DOI: 10.1039/C4CP05007J.

3 C. Yeh, J. Ho, *Phys. Chem. Chem. Phys.*, 2015, DOI: 10.1039/C5CP00212E.

4 J-X. Zhao, Y-H. Ding, *Mater. Chem. Phys*., 2008, **110**, 411.

5 S. Nigam, C. Majumder, *ACS Nano*, 2008, **2**, 1422.

6 Y-H. Zhang, K-G. Zhou, X-C. Gou, K-F. Xie, H-L. Zhang, Y. Peng, *Chem. Phys. Lett.,* 2010, **484**, 266.

7 A. Ahmadi Peyghan, A. Soltani, A. Allah Pahlevani, Y. Kanani, S. Khajeh, *Appli. Surf. Sci.*, 2013, **270**, 25.

8 P. Rochana, J. Wilcox, *Surf. Sci.,* 2011, **605**, 681.

9 Q. Yuan, Y-P. Zhao, L. Li, T. Wang, *J. Phys. Chem. C*, 2009, **113**, 6107.

10 J. Beheshtian, Z. Bagheri, M. Kamfiroozi, A. Ahmadi, *Microelectron J.*, 2011, **42**, 1400.

11 S. Sinthika, E. Mathan Kumar and Ranjit Thapa, *J. Mater. Chem. A*, 2014, **2**, 12812.

12 M. Bezi Javan, *Surf. Sci.,* 2015, **635**, 128.

13 R.J. Baierlea , T.M. Schmidt, A. Fazzio, *Solid State Communications*, 2007, **142**, 49.

14 Z. Liu, Q. Xue, T. Zhang, Y. Tao, C. Ling, M. Shan, *J. Phys. Chem. C*, 2013, **117**, 9332.

15 Q. Dong, X.M. Li, W.Q. Tian, X-R. Huang, C-C. Sun, *J. Mole. Struct.(Theochem)*, 2010, **948**, 83.

16 B. Gao, J-x. Zhao, Q-h. Cai, X-g. Wang, X-z. Wang, *J. Phys. Chem. A*, 2011, **115**, 9969.

17 S. Lin, X. Ye, R.S. Johnson, H. Guo, *J. Phys. Chem. C*, 2013, ***117*** **(33)**, 17319.

18 A. Nishiwaki, T. Oku, I. Narita, *Sci. Tech. Adv. Mater.*, 2004, **5**, 629.

19 T. Oku, K. Hiraga, T. Matsuda, *Mater. Trans*., 2008, **49**, 2461.

20 C. Huang, W. Ye, Q. Liu, X. Qiu, *ACS Appl. Mater. Interfac.*, 2014, dx.doi.org/10.1021/am5037737.

21 V.V. Pokropivny, V.V. Skorokhod, G.S. Oleinik, A.V. Kurdyumov, T.S. Bartnitskaya, A.V. Pokropivny, A.G. Sisonyuk, D.M. Sheichenko, *J. Solid State Chem.*, 2000, **154**, 214.

22 J. Guo-Qiang, C. Xin, H. Zheng, *Chin. Phys. Lett.*, 2009, **26**, 033601.

23 A.V. Pokropivny, *Diamond & Related Mater*., 2006, **15**, 1492.

24 A. Soltani, M.T. Baei, M. Ramezani Taghartapeh, E. Tazikeh Lemeski, S. Shojaee, *Struct Chem*, 2015, **26**, 685.

25 A. Ahmadi Peyghan, H. Soleymanabadi, *Curr. Sci.*, 2015, **108**, 1910.

26 S. Yourdkhani, T. Korona, N.L. Hadipour, *J. Phys. Chem. A*, 2015, **119**, 6446.

27 T. Oku, A. Nishiwaki, I. Narita, *Sci. Tech. Adv. Mater*., 2004, **5**, 635.

28 J. M. Matxain, L. A. Eriksson, J. M. Mercero, X. Lopez, M. Piris, and J. M. Ugalde, J. Poater, E. Matito and M. Sola, *J. Phys. Chem. C*, 2007, **111**, 13354.`

29 F. Li, Y. Zhang, H. Chen, *Phys. E*, 2014, **56**, 216.

30 A. Bahrami, S. Seidi, T. Baheri, M. Aghamohammadi, *Superlattic. Microstruct*., 2013, **64**, 265.

31 N. Injan, J. Sirijaraensreb, J. Limtrakul, *Phys. Chem. Chem. Phys*., 2014, **16**, 23182.

32 N.L. Hadipour, A. Ahmadi Peyghan, H. Soleymanabadi, *J. Phys. Chem. C,* 2015, ***119*** **(11)**, 6398.

33 A. Soltani, M.T. Baei, M. Mirarab, M. Sheikhi, E. Tazikeh Lemeski, *J. Phys. Chem. Solids*, 2014, **75**, 1099.

34 M.W. Schmidt, K.K. Baldridge, J.A. Boatz, S.T. Elbert, M.S. Gordon, J.H. Jensen, S.Koseki, N. Matsunaga, et al., *J. Comput. Chem*., 1993, **11**, 1347.

35 J.P. Perdew, K. Burke, M. Ernzerhof, *Phys. Rev. Lett*., 1996, **77**, 3865.

36 S-l. Tang, Y-j. Liu, H-x. Wang, J-x. Zhao, Q-h. Cai, X-z. Wang, *Diamond & Related Materials*, 2014, **44**, 54.

37 Q. Sun, Z. Li, D.J Searles, Y. Chen, G. Lu, A. Du, *J. Am. Chem. Soc*., 2013, **135**, 8246.

38 F. Tournus, J.-C. Charlier, *Phys. Rev. B*, 2005, **71**, 165421.

39 M.T. Baei, M. Ramezani Taghartapeh, E. Tazikeh Lemeski, A. Soltani, *Superlattic. Microstruct.* 2014, **72**, 370.

40 R.G. Parr, R.A. Donelly, M. Levy, W.E. Palke, *J. Chem. Phys.*, 1978, **68**, 3801.

41 R.G. Parr, L. Szentpaly, S. Liu, *J. Am. Chem. Soc*., 1999, **121**, 1922.

42 T. Koopmans, *Physica*, 1933, **1**, 104.

43 Z. Li, C-Y. Wang, *Chem. Phys*., 2006, **330**, 417.

44 J. Beheshtian, M.T. Baei, A. Ahmadi Peyghan, *Surf. Sci*., 2012, **606**, 981.

45 D.R. Lide, Handbook of Chemistry and Physics, CRC, Florida, 1992.

46 H.Y. Wu, X.F. Fan, J-L. Kuo, W-Q. Deng, *Chem. Commun*., 2010, **46**, 883.

47 M.T. Baei, *Comput. Theor. Chem*., 2013, **1024**, 28.

48 J. Beheshtian, A. Ahmadi Peyghan, M. Noei, *Sensors and Actuators B*, 2013,**181**, 829.

49 N. M. O'Boyle, A. L. Tenderholt, K. M. Langner, *J. Comput. Chem*. 2008, **29**, 839.

50 A. Ahmadi Peyghana, S.F. Rastegar, N.L. Hadipour, *Phys. Lett. A*, 2014, **378**, 2184.

51 J. Beheshtian, A. Ahmadi Peyghan, Z. Bagheri, *Sensors and Actuators B*, 2012, **171-172**, 846.

52 Z. Bolboli Nojini, S. Samiee, *J. Phys. Chem. C*, 2011, **115**, 12054.

53 P.K. Chattaraj, U. Sarkar, D.R. Roy, *Chem. Rev*. 2006, **106**, 2065.

54 R.G. Parr, L.V. Szentpály, S. Liu, *J. Am. Chem. Soc*. 1999, **121**, 1922.

55 S. Armaković, S.J. Armaković, J.P. Šetrajčić, S.K. Jaćimovski, V. Holodkov, *J Mol Model*, 2014, **20**, 2170.

56 V.V. Pokropivny, V.V. Skorokhod, G.S. Oleinik, A.V. Kurdyumov, T.S. Bartnitskaya, A.V. Pokropivny, A.G. Sisonyuk, D.M. Sheichenko, *J. Solid State Chem*., 2000, **154**, 214.

57 F. Jensen, H. Toftlund, *Chem. Phys. Lett*., 1993, **201**, 89.

58 H. Ullah, A-u-H. Ali Shah, S. Bilal, K. Ayub, *J. Phys. Chem. C*, 2013, **117**, 23701.

Fig. 1. Optimized structures and density of state spectra of CO and $B_{12}N_{12}$ nano-clusters.

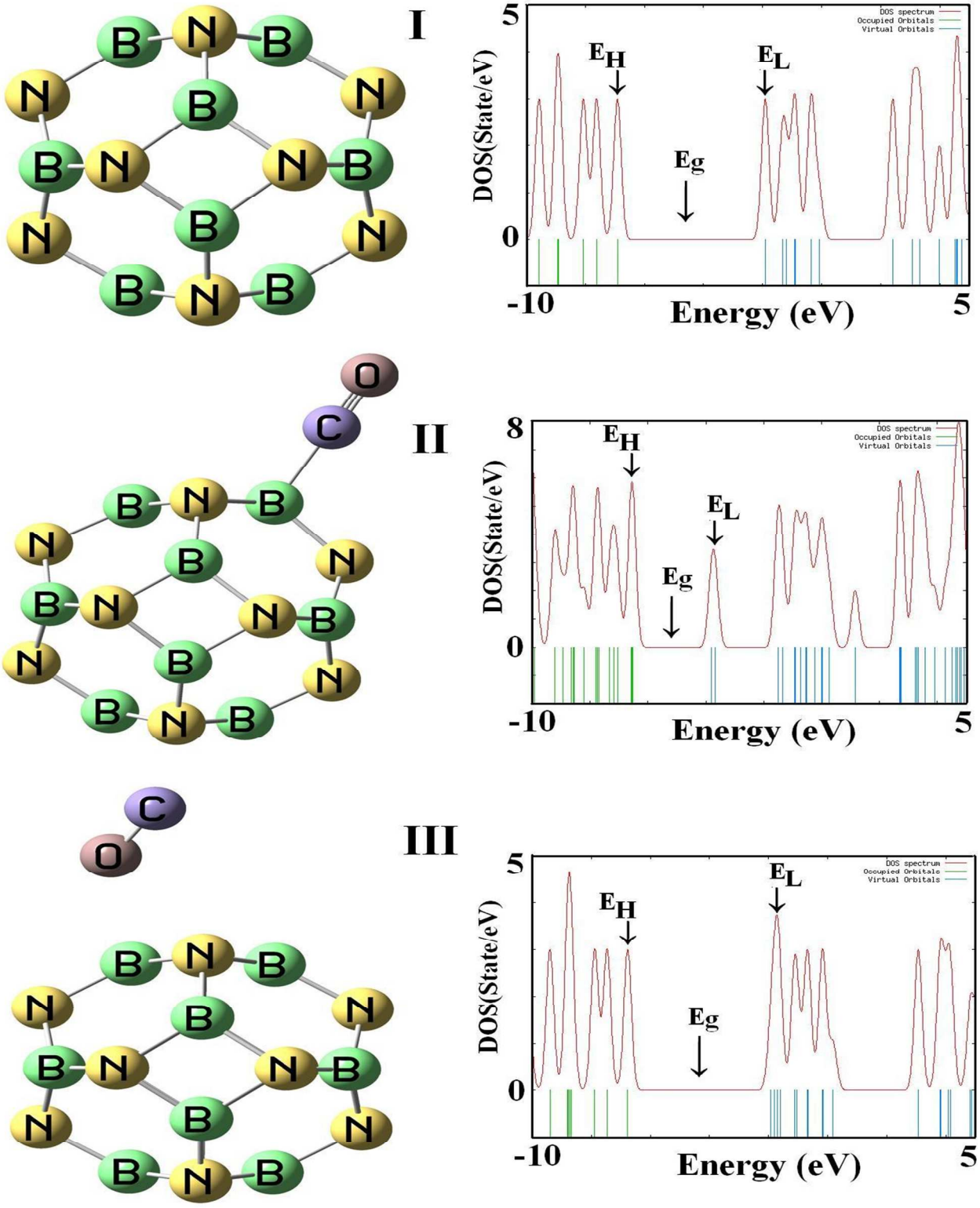

Fig. 2. Optimized structures, infrared and density of state spectra of $B_{11}XN_{12}$ nano-clusters.

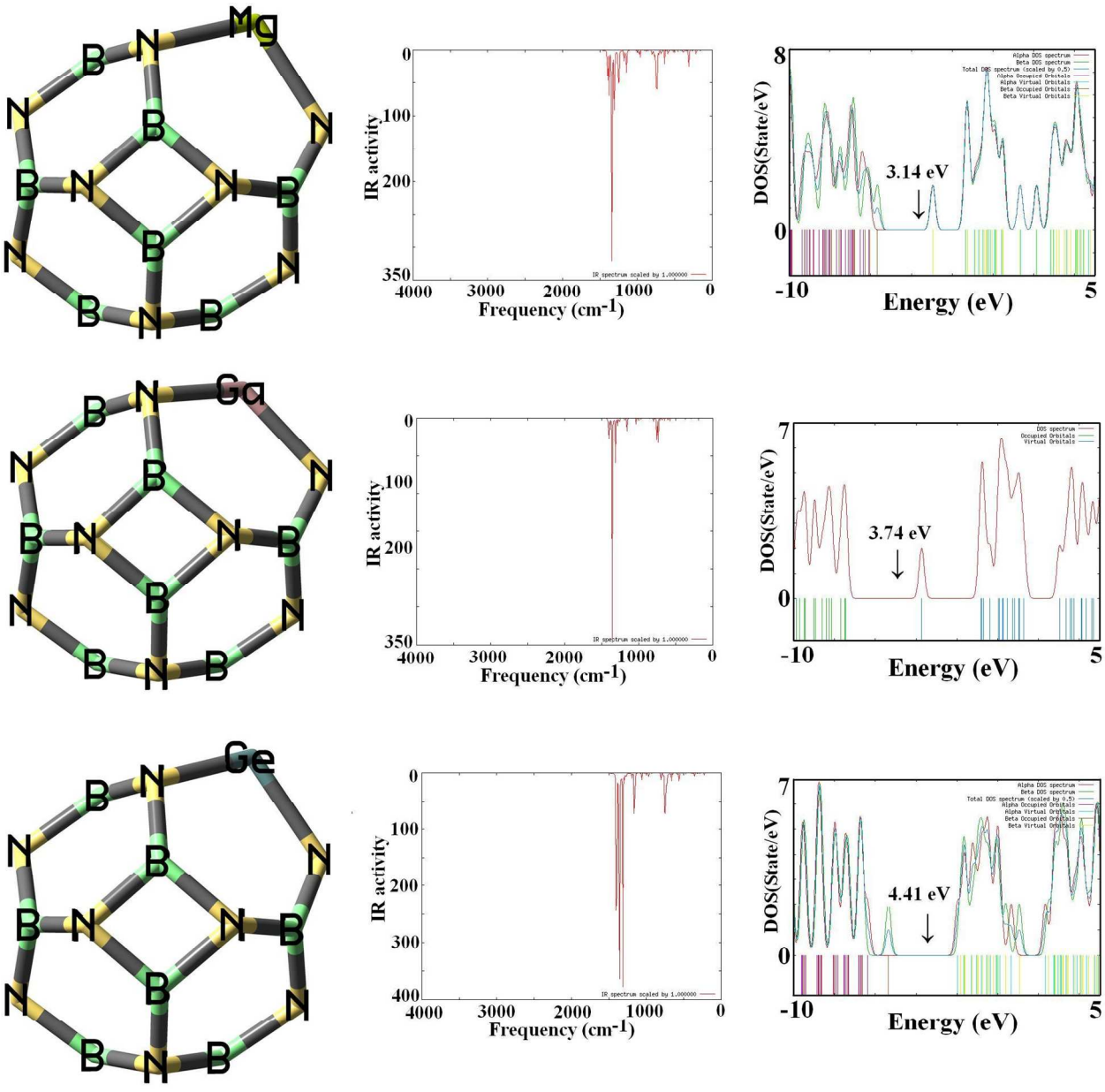

Fig. 3. Crucial transition states of $B_{11}XN_{12}$ structures, where the largest component coefficient is marked.

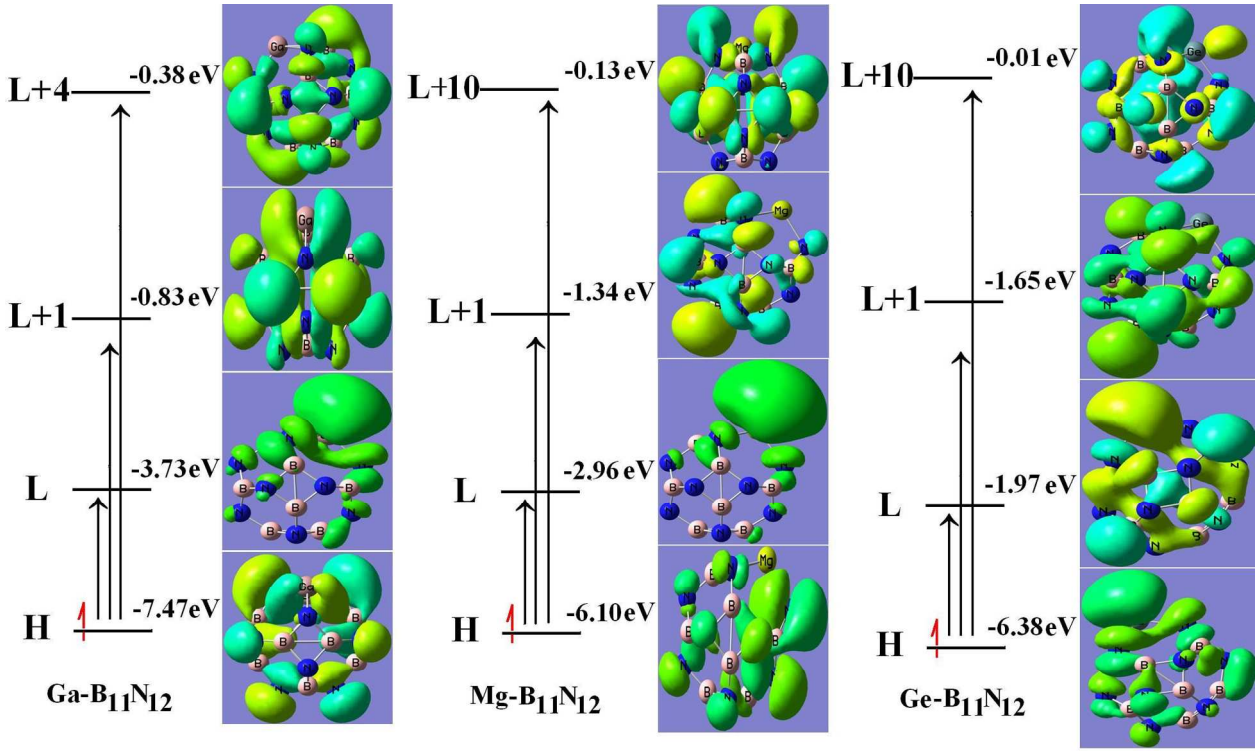

Fig. 4. Optimized structures, infrared and density of state spectra of $B_{11}MgN_{12}$ nano-clusters interacted with CO molecule.

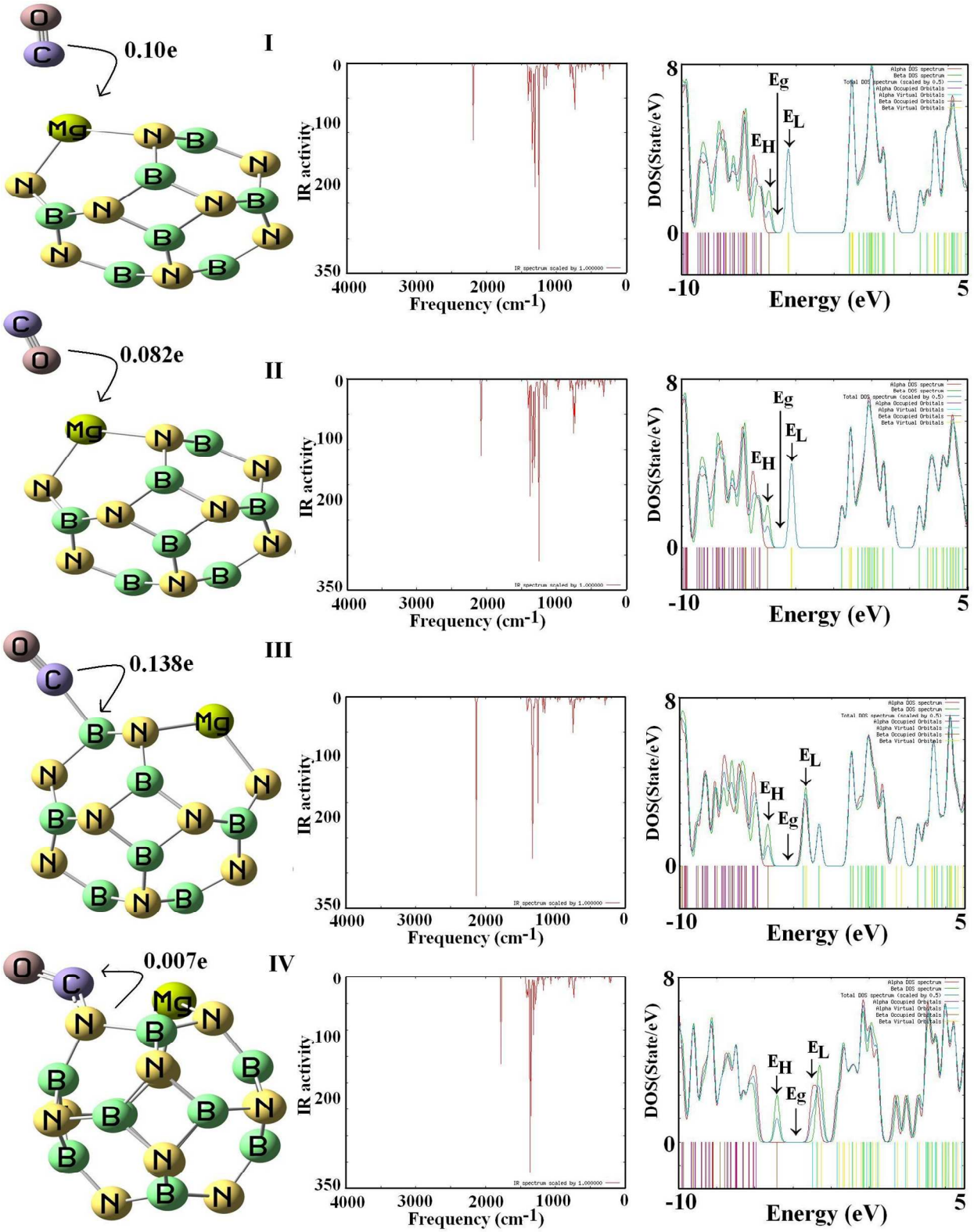

Fig. 5. Optimized structures, infrared and density of state spectra of $B_{11}GaN_{12}$ nano-clusters interacted with CO molecule.

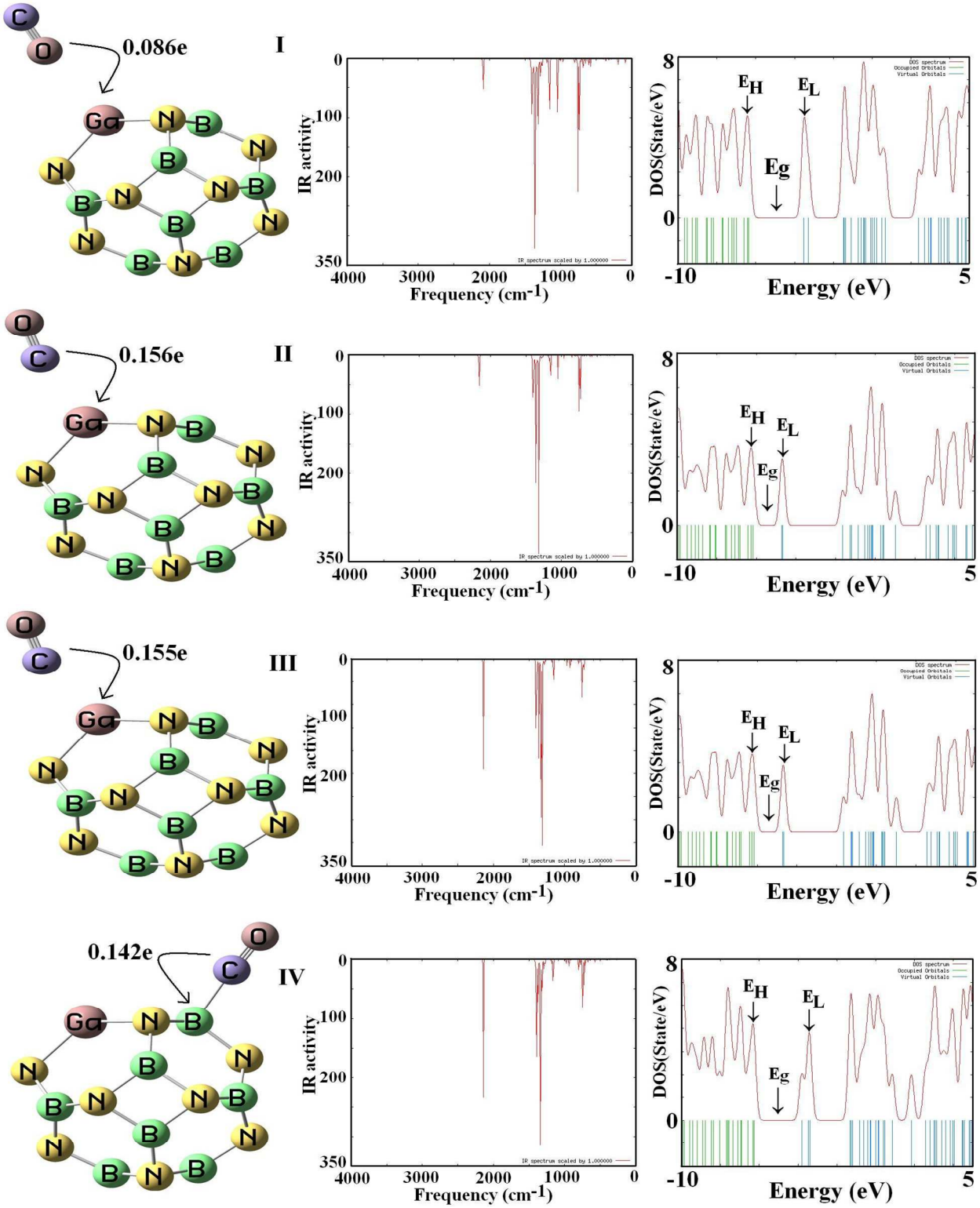

Fig. 6. Optimized structures, infrared and density of state spectra of $B_{11}GeN_{12}$ nano-clusters interacted with CO molecule.

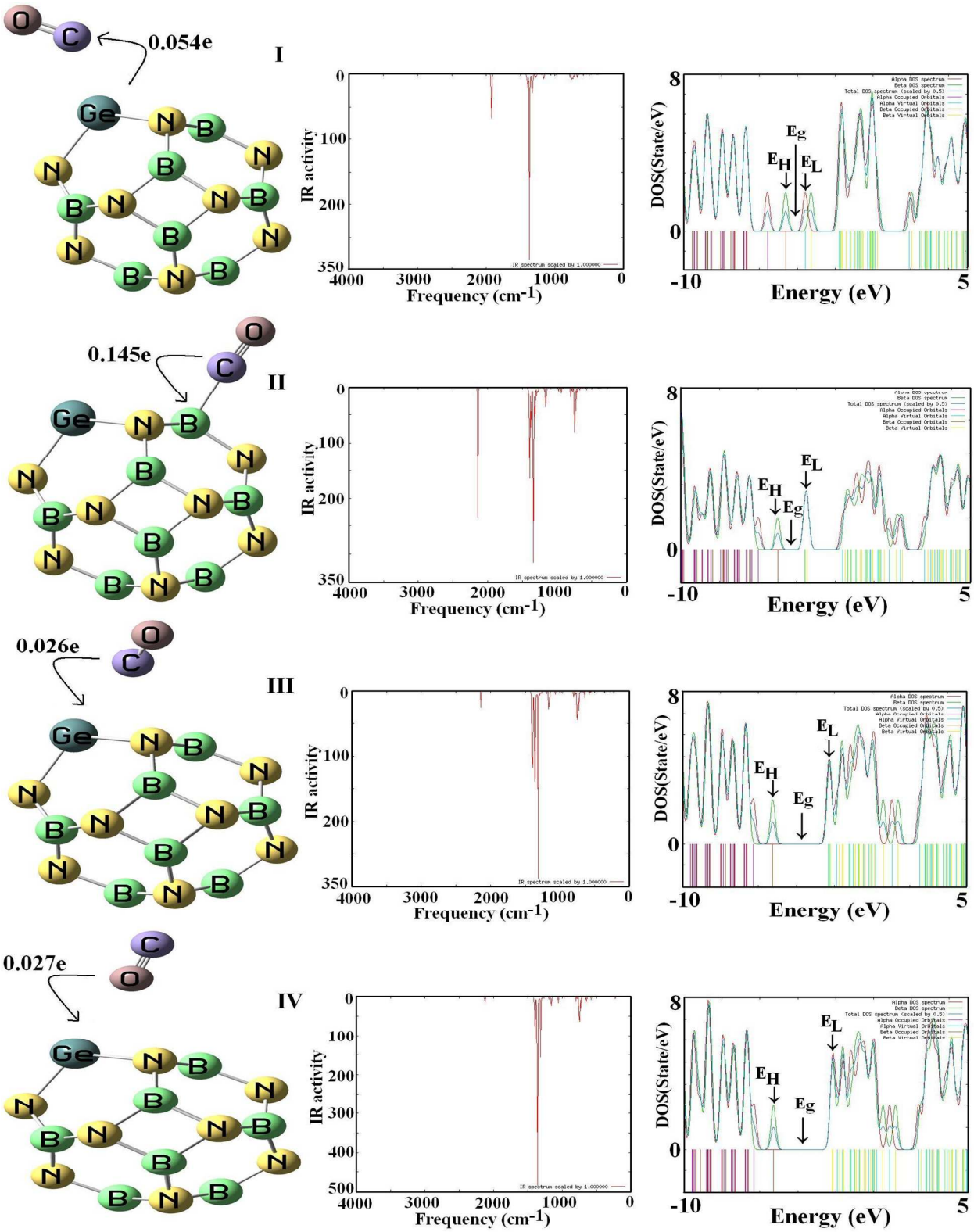

Fig. 7. Crucial transition states of the $B_{11}XN_{12}$ structures interacted with CO, where the largest component coefficient is marked.

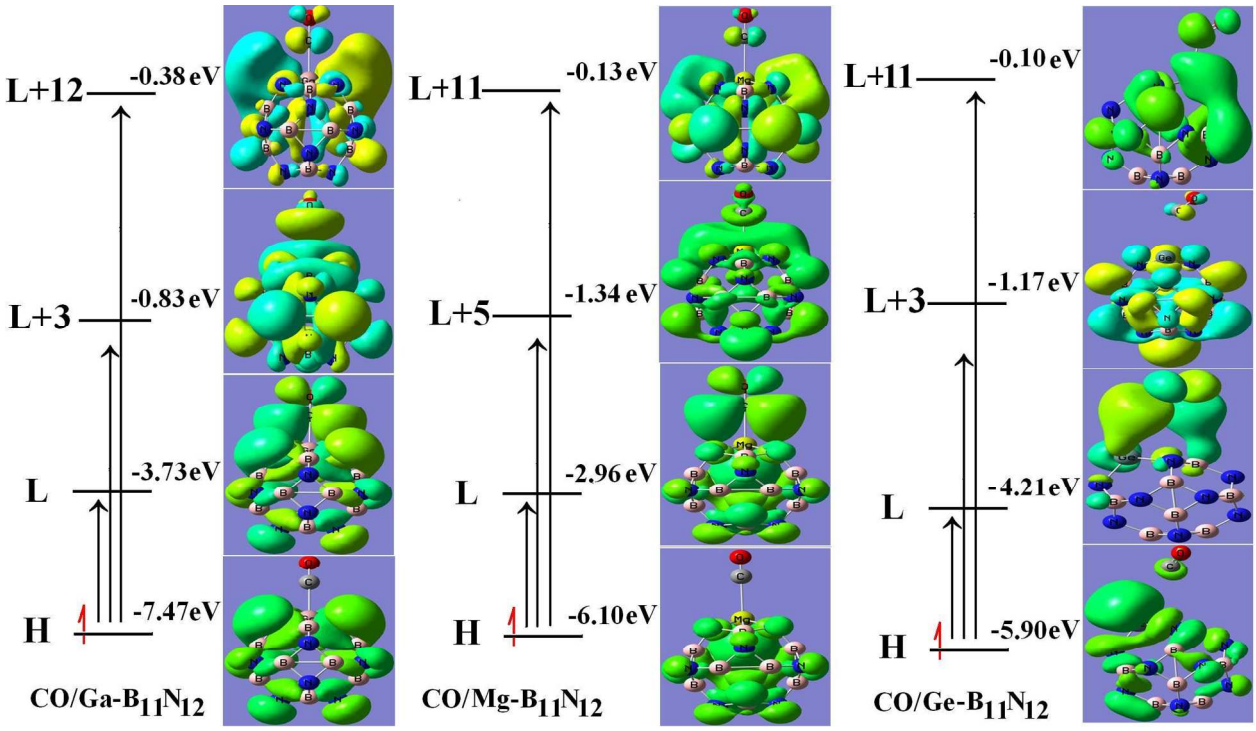

Fig. 8. Calculated electrostatic potentials with a density isosurface of 0.0004 electrons au^{-3}. The scale bar is in atomic units.

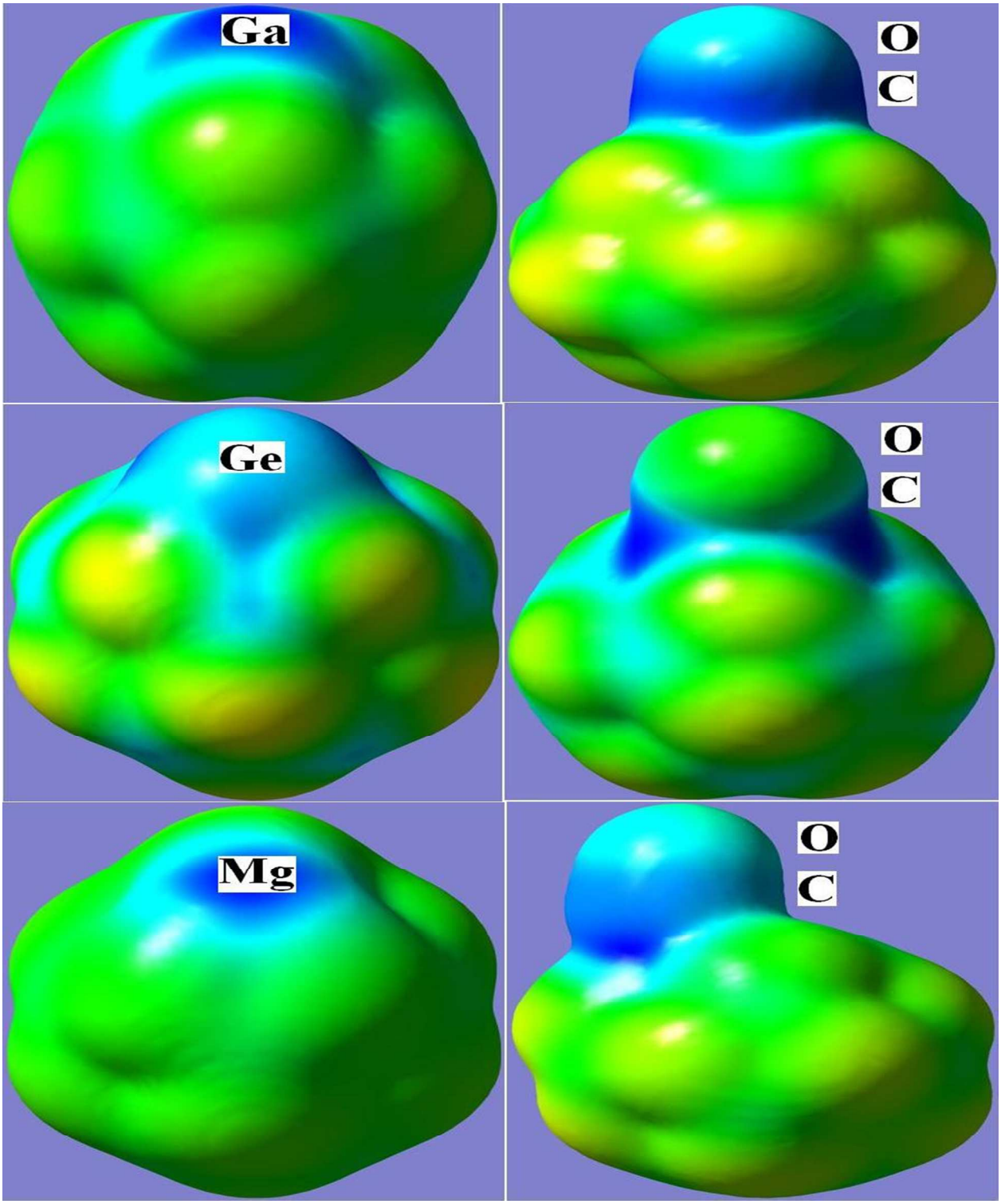

Table 1 Calculated bond length, adsorbate-surface distance D/Å, adsorption energy E_{ad}/eV, HOMO energies (E_{HOMO}/eV), LUMO energies (E_{LUMO}/eV), dipole moment (DM/Debye), Fermi level energies (E_F/eV) and HOMO-LUMO energy gap (E_g/eV) for pure $B_{12}N_{12}$ nano-cluster.

system	E_{ad}/eV	D/Å	C-O/Å	B-N/ Å	E_{HOMO}/eV	E_g/eV	E_{LUMO}/eV	ΔE_g%	E_F/eV	DM/Debye
CO	-	-	1.1386	-	-8.87	7.03	-1.84	-	-5.36	0.226
I	-	-	-	1.493	-6.91	5.0	-1.91	-	-4.41	0.00
II	-0.27	1.655	1.136	1.563	-6.52	2.71	-3.81	-45.8	-5.17	3.62
III	-0.06	3.176	1.139	1.495	-6.90	4.81	-2.09	-3.80	-4.50	0.182

Table 2 The obtained structural parameters for a single CO adsorption over the pure and $B_{11}XN_{12}$ nano-clusters.

system	$R_{C=O}$	R_{Ga-N}	R_{Ge-N}	R_{Mg-N}	R_{N-Ga-N}	R_{N-Ge-N}	R_{N-Mg-N}
$GaB_{11}N_{12}$	-	1.921	-	-			
State I	1.144	1.923	-	-	117.889	-	-
State II	1.133	1.938	-	-	114.828	-	-
State III	1.132	1.937	-	-	114.707	-	-
State IV	1.137	1.910	-	-	120.488	-	-
$GeB_{11}N_{12}$	-		1.946				
State I	1.164	-	1.922	-	-	107.243	-
State II	1.140	-	1.947	-	-	105.975	-
State III	1.137	-	1.934	-	-	107.591	-
State IV	1.138	-	1.890	-	-	105.814	-
$MgB_{11}N_{12}$	-			2.079			
State I	1.132	-	-	2.098	-	-	105.671
State II	1.138	-	-	2.064	-	-	105.079
State III	1.146	-	-	2.088	-	-	110.126
State IV	1.203	-	-	2.010	-	-	106.710

Table 3 Calculated bond length, adsorbate-surface distance D/Å, adsorption energy E_{ad}/eV, HOMO energies (E_{HOMO}/eV), LUMO energies (E_{LUMO}/eV), work function (Φ/eV), dipole moment (DM/Debye), Fermi level energies (E_F/eV) and HOMO-LUMO energy gap (E_g/eV) for X-doped $B_{11}N_{12}$ nano-cluster.

system	E_{ad}/eV	D/Å	E_{HOMO}/eV	E_g/eV	E_{LUMO}/eV	ΔE_g%	E_F/eV	Φ/eV	DM/Debye
$GaB_{11}N_{12}$	-	-	-7.47	3.74	-3.73	-	-5.60	1.87	2.654
State I	-0.200	2.511	-6.36	2.83	-3.53	24.33	-4.95	1.42	6.492
State II	-0.657	2.148	-6.17	1.45	-4.72	61.23	-5.44	0.72	6.478
State III	-0.668	2.148	-6.19	1.45	-4.70	60.16	-5.44	0.74	2.556
State IV	-0.221	1.671	-6.28	5.023	-3.81	33.96	-5.04	1.23	4.562
$GeB_{11}N_{12}$	-	-	-6.38	4.41	-1.97	-	-4.18	2.21	1.673
State I	-0.132	2.179	-4.423	2.88	-1.54	-34.74	-2.98	1.44	1.577
State II	-0.067	3.476	-3.981	2.34	-1.64	-46.82	-2.81	1.17	1.188
State III	-0.163	1.685	-6.288	4.93	-1.36	11.68	-3.83	2.47	1.8203
State IV	-0.059	3.466	-6.270	4.73	-1.54	7.26	-3.91	2.37	1.840
$MgB_{11}N_{12}$	-	-	-6.10	3.14	-2.96	-	-4.53	1.57	5.249
State I	-0.589	2.270	-5.86	1.44	-4.42	54.14	-5.14	0.72	7.246
State II	-0.356	2.351	-5.90	4.741	-4.21	46.18	-5.0	0.79	5.38
State III	-0.871	1.681	-5.92	2.93	-2.99	6.69	-4.45	1.46	6.85
State IV	-0.073	1.358	-5.90	2.41	-3.49	23.25	-4.70	1.21	4.061

Table 4 Calculated the quantum molecular discriptors for CO molecule interacting with $B_{11}XN_{12}$ nano-cluster.

system	I/eV	A/eV	η/eV	μ/eV	ω/eV	χ/eV	S/eV
$GaB_{11}N_{12}$	7.47	3.73	1.87	-5.6	8.38	5.6	0.27
State I	6.16	1.244	2.46	-3.70	2.79	3.70	0.20
State II	6.38	1.383	2.49	-3.88	3.02	3.88	0.20
State III	6.57	1.483	2.54	-4.03	3.18	4.03	0.196
State IV	6.310	1.287	2.51	-3.80	2.87	3.80	0.199
State V	6.482	1.197	2.64	-3.84	2.79	3.84	0.189
$GeB_{11}N_{12}$	6.38	1.97	2.21	-4.18	3.95	4.18	0.226
State I	4.423	1.545	1.44	-2.98	3.09	2.98	0.347
State II	3.981	1.636	1.17	-2.81	3.63	2.81	0.426
State III	6.288	1.363	2.46	-3.83	2.97	3.83	0.203
State IV	6.270	1.540	2.37	-3.91	3.22	3.91	0.211
State V	6.328	1.212	2.56	-3.77	2.78	3.77	0.195
$MgB_{11}N_{12}$	6.10	2.96	1.57	-4.53	6.53	4.53	0.318
State I	5.901	1.086	2.41	-3.49	2.53	3.49	0.207
State II	5.948	1.207	2.37	-3.58	2.70	3.58	0.210
State III	5.958	0.990	2.48	-3.47	2.43	3.47	0.201
State IV	6.178	1.318	2.43	-3.75	2.89	3.75	0.205
State V	6.077	0.903	2.59	-3.49	2.35	3.49	0.193

Table 5 Selected excitation energies (eV, nm), oscillator strength (f), and relative orbital contributions of calculated at the PBE method.

Methods	Energy/eV	Wavelength/ nm	Oscillator Strength (*f*)	Assignment
Ga doping	2.44	508	0.0040	H-1 → [a]L (100%)
	2.66	465	0.0070	H-2 → L (100%)
State I	2.85	435	0.0016	H → L+1 (100%)
	2.90	428	0.0002	H-1 → L (100%)
State II	1.52	817	0.0084	H → L (99%)
	1.54	804	0.0003	H-1 → L (99%)
State III	1.51	818	0.0035	H → L (96%)
	1.53	806	0.0003	H-1 → L (99%)
State IV	2.54	488	0.0004	H-1 → L (100%)
	2.82	439	0.0105	H-2 → L (99%)
Mg doping	0.66	1891	0.0010	H → L (100%)
	1.17	1061	0.0006	H-1 → L (99%)
State I	0.71	1740	0.0011	H → L (100%)
	1.22	1013	0.0008	H-1 → L (99%)
State II	0.70	1780	0.0012	H-1 → L (99%)
	1.21	1024	0.0008	H-2 → L (64%)
State III	0.75	1646	0.0005	H-1 → L (99%)
	1.12	1101	0.0007	H-2 → L (98%)
State IV	1.47	840	0.0016	H-1 → L (100%)
	1.76	703	0.0020	H-2 → L (100%)
Ge doping	1.352	917	0.0020	H-1 → L (100%)
	1.433	865	0.0014	H-2 → L (100%)
State I	1.973	628	0.0001	H → L (98%)
	2.09	593	0.0032	H-1 → L (100%)
State II	1.46	848	0.0006	H-1→ L (100%)
	1.61	772	0.0021	H-2 → L (100%)
State III	1.41	878	0.0020	H-1→ L (100%)
	1.48	835	0.0011	H-2 → L (100%)
State IV	1.40	887	0.0020	H-1 → L (100%)
	1.47	842	0.0012	H-2 → L (100%)

[a]H and L mean the highest occupied (HOMO) and lowest unoccupied molecular orbitals (LUMO), respectively.

The influence of CO adsorption over the electronic and optical properties of $B_{11}XN_{12}$ nano-cluster has been studied by DFT calculations.